International Food Research Journal 18: 287-302 (2011)

Effect of palm pressed fiber (PPF) surface treatment on the properties of rice starch films

Phattaraporn, T., Waranyou, S. and *Thawien, W.

Starch and Plant Fiber Research Unit (SPF-RU), Department of Material Product Technology
Prince of Songkla University, Hat Yai, Songkhla, 90112, Thailand

Abstract: The biodegradable rice starch (RS) films reinforced with different concentration of palm pressed fiber (PPF) silane treatments (10, 20, 30 and 40% glysidoxy propyltriethoxy silane/PPF) and content of treated PPF were investigated. Higher tensile strength (TS), water vapor permeability (WVP) and thermal properties of biodegradable RS films were obtained as silane treated PPF was applied. Increasing concentration of silane and content of silane treated PPF resulted in increased TS and WVP but decreased elongation at break (E). The thermal properties behavior of biodegradable RS films reinforced with treated and untreated PPF were investigated by means of Dynamic mechanical thermal analysis (DMTA), Differential scanning calorimetry (DSC) and Thermogravimetric analysis (TGA). The glass temperature (Tg) shifted towards higher temperatures with increasing concentration of silane, which can be restriction of the mobility of starch chain due to the establishment of strong interactions between RS and treated PPF. The maximum improvement of RS films in the mechanical and thermal properties obtained when 40% of silane treated PPF films was applied. These results pointed out that the interfacial interactions improved the filler compatibility, mechanical and thermal properties.

Keywords: rice starch film, palm pressed fiber, surface treatment, alkaline treatment, silane treatment

Introduction

Most synthetic films are petrochemical-based and non-biodegradable; it takes a several hundred years to degrade petroleum-based synthetic plastics, which have caused serious solid waste contamination in the world (Park et al., 2002). In contrast, edible films use renewable resources as raw materials and are biodegradable, making them more compatible with the environment. Usually biodegradable and edible films include lipids, proteins and carbohydrates such as cellulose, starch and there derivatives in their formulation (Rodriguez et al., 2006). Starch is a low cost material in comparison to most synthetic plastics and is readily available. Starch has been investigated widely for the potential manufacture of products such as water-soluble pouches for detergents and insecticides, flushable liners and bags, and medical delivery systems and devices (Fishman et al., 2000). Rice is the most widely consumed basic food in the world. Each year over 500 million tons of rice is harvested, providing sustenance to many countries and people throughout the world. The unique properties of rice starches are found in its many varieties (Bourtoom and Chinnan, 2008). Rice starch and its major components, amylose and amylopectin, are biopolymers, which are attractive raw materials for used as barriers in packaging materials They have been used to produce biodegradable films to partially or entirely replace plastic polymers because of its low cost and renewability, as well as possessing good mechanical properties (Xu et al., 2005). However, compared to the common thermoplastics, biodegradable products based on starch (Lourdin et al., 1995; Mali and Grossmann, 2003), unfortunately, still reveal many disadvantages such as low mechanical properties and efficient barrier against low polarity compounds (Kester and Fennema, 1986). The disadvantages mainly attributed to the highly hydrophilic character of starch polymers (Santayanon and Wootthikanokkhan, 2003). One approach these problem is the use of fibers as reinforcement for starch (Ma et al, 2008). Natural fiber-reinforced composites have many advantages such as light weight, reasonable strength and stiffness, renewable and biodegradable (Demir et al., 2006; Kunanopparat et al., 2008). Various types of fillers have been tested such as potato pulp based microfibrils (Dufresne et al., 2000; Dufresne and Vignon, 1998), bleached leaf wood fibers (Averous and Boquillon, 2004; Funke et

*Corresponding author.
Email: *thawean.b@psu.ac.th*
Tel: +(66) 74446731, Fax: +(66) 74212889

al., 1998), bleached eucalyptus pulp fibers (Curvelo et al., 2001), wood pulp (De Carvalho et al., 2002), softwood aspen (Low et al., 2007), Jute, Hemp and flax fibers (Park et al., 2006; Soykeabkaew et al., 2004; Wollerdorfer and Bader, 1998) tunicin whiskers (Angles and Dufresne, 2000; Angles and Dufresne, 2001) and oil palm fibers (Sreekala and Thomas, 2003). However, the performance and properties of composite materials depend on the properties of the individual components and their interfacial compatibility. To ensure appropriate interfacial interactions their surface properties must be modified accordingly. The surface is influenced by polymer morphology, extractive chemicals and processing conditions (Bledzki and Gassan, 1999). Chemical treatment of cellulosic materials usually changes the physical and chemical structure of the fiber by reacting with the OH group of the cellulose. There are reports that chemically treated palm fibers are more stable and can withstand heat to a greater extent compared with untreated fibers (Sreekala and Thomas, 2003) during the course of thermal cycling. In previous work (Bourtoom and Chinnan, 2008; Wittaya, 2009) a rice starch edible film was developed. It has been observed that the functional properties e.g., the film ductility and the barrier properties of rice starch film are generally poor. The objective of this work was to investigate the influence of palm pressed fiber (PPF) surface treatments (silane treatment) on the physical, mechanical and thermal properties of rice starch film.

Materials and Methods

Materials

Native rice starch (Thai Flower brand) used was obtained from Bangkok Starch Industrial Co. Ltd. and had a moisture content of about 14g/100g sample (determined in triplicate by vacuum drying at 70°C and < 1 mmHg pressure for 24 h, EYELA™, Model VOS-300VD, Japan) and peak viscosity (8g/100g sample solid) of 500 BU (Brabender unit, Model VISKOGRAPH, Germany). Native rice starch (Thai Flower brand) was obtained from Bangkok Starch Industrial Co. Ltd. Commercial grade sorbitol was obtained from Vidyasom Co. Ltd. (Thailand).

Chemical reagents

The coupling agents (glysidoxypropyl trimethoxy silane) were supplied by Sigma-Aldrich Chemie, Damstadt, Germany. Analytical grade (AR) Magnesium Chloride, Magnesium Nitrate, Sodium Chloride, Potassium Nitrate and Sodium Sulfate for saturated salt solutions (at 33% RH, 50% RH, 75% RH, 90% RH and 98% RH, respectively) were purchased from High Science Co. Ltd. (Thailand). Nitric acid 10%, Sodium Hypochlorite 10%, Sulfuric acid 64%, Acetone, Acetic acid were purchased from KSP Co. Ltd. (Thailand).

Preparation of palm presses fiber and surface treatment

Palm pressed fiber (PPF) were prepared by acid treatment (10% HNO_3) at 90°C for 1 h and bleaching the produced pulp using the sodium hypochloride bleaching method. Then, was chopped (420 µm) and treated by silane coupling agents (10, 20, 30 and 40% of PPF). The surface treatments of dried PPF fibers were carried out in the acetone solution of silane. Fibers (5 g) and silane (0.5 g) were put in flask with the proper volume of acetone. After agitation for half and hour, the flask was sealed with a parafin film and kept for 12 h at room temperature. Then the samples were first washed with acetone to remove compound, and dried at 80°C in an oven to constant weight (Shih, 2006).

Film preparation

Starch solution with concentration of 3% (w/v) was prepared by dispersing rice starch in distilled water and heating the mixtures with stirring until it gelatinized (85°C for 5 min), and then cooling to 45± 2°C. The solution was filtered through a polyester screen (mesh no.140 with mesh opening of 106 µm) by vacuum aspiration to remove any small lumps in the solution. Sorbitol was added 50% of starch solution. Subsequently, the treated PPF dispersion was added at 10, 20, 30 and 40% of sorbitol and stirred for 20 min. After mixing, the mixer was degassed under vacuum cast onto flat, leveled non-stick tray to set. Once set, the tray were held at 55°C for 10 h undisturbed, and then cooled to ambient temperature before peeling the films off the plates. All treatments were made in triplicate.

Film testing

Conditioning

All films were conditioned prior to subjecting them to permeability and mechanical tests according to the Standard method, D618-61 (ASTM, 1993a). Films used for testing water vapor permeability (WVP), tensile strength (TS), and elongation (E) were conditioned at 60% RH and 27+2°C by placing them in desiccators over a saturated solution of $Mg(NO_3)_2 .6H_2O$ for 72 h or more. For other tests, film samples were transferred to plastic bags after peeling and placed in desiccators.

Film thickness

Thickness of the films was measured with a precision digital micrometer (Digimatic Indicator, Mitutoyo Corporation, Japan) to the nearest 0.0001 (±5%) at five random locations on the film. Mean thickness values for each sample were calculated and used in water vapor permeability (WVP) and tensile strength (TS) calculations.

Water vapor permeability (WVP)

The gravimetric Modified Cup Method based on ASTM E96-92 (McHugh et al, 1993) was used to determine the WVP of films. The test cups were filled with 20g of Silica gel (desiccant) to produce a 0% RH below the film. A sample was placed in between the cup and the ring cover of each cup coated with silicone sealant (high vacuum grease, Lithelin, Hannau, Germany) and held with four screws around the cup's circumference. The air gap was at approximately 1.5cm between the film surface and desiccant. The water vapor transmission rates (WVTR) of each film were measured at 60+ 2% RH and 25+2°C. After taking the initial weight of the test cup, it was placed into a growth chamber with an air velocity rate of 125 m/min (Model KBF115, Contherm Scientific, Lower Hutt, New Zealand). Weight gain measurements were taken by weighing the test cup to the nearest 0.0001g with an electronic scale (Sartorious Corp.) every 3 h for 18 h. A plot of weight gained versus time was used to determine the WVTR. The slope of the linear portion of this plot represented the steady state amount of water vapor diffusing through the film per unit time (g/h). The WVTR was expressed in gram units, per square meter, per day. Steady state over time (slope) yielded a regression coefficient of 0.99 or greater. Six samples per treatment were tested. The WVP of film was calculated by multiplying the steady WVTR by the film thickness and dividing that by the water vapor pressure difference across the film.

Tensile strength and elongation at the break (TS and E).

Tensile strength was measured with a LLOYD Instrument (Model LR30K, LLOYD Instruments Ltd., Hampshire, England) as per ASTM D882-91 Standard Method (ASTM, 1993b). Ten samples, 2.54 cm x 12cm, were cut from each film. Initial grip separation and crosshead speed were set at 50mm and 50mm/min, respectively. Tensile strength was calculated by dividing the maximum force by the initial specimen cross-sectional area, and the percent elongation at the break was calculated as follows:

$$E = 100 \text{ X } (d_{after} - d_{before})/d_{before}$$

Where, d was the distance between grips holding the specimen before or after the break of the specimen.

Color

A CIE colorimeter (Hunter associates laboratory, Inc., VA. USA) was used to determine the film L*, a*, and b* color value [(L* = 0 (black) to 100 (white); a* = -60 (green) to +60 (red); and b* = -60 (blue) to +60 (yellow)]. The standard plate (calibration plate CX0384, L*= 92.82, a*= -1.24, and b*= 0.5) was used as a standard. Color (means of five measurements at different locations on each specimen) was measured on 10cm x 10cm segment of film. Total color difference (ΔE*ab), hue angle (H), and chroma (C) were calculated using the following equation:

ΔL* = L* sample – L* standard, Δa* = a* sample - a* standard, Δb* = b* sample - b* standard
ΔEab* = [(ΔL*) 2 + (Δa*) 2 + (Δb*) 2]0.5
C = [(a*) 2 + (b*) 2] 0.5
H = tan-1 (b*/a*) when a* > 0 and b* > 0
H = 180o + tan-1 (b*/a*) when a* < 0
H = 360 o + tan-1 (b*/a*) when a* > 0 and b* < 0

Prior to taking color measurements, film specimens were pre-conditioned at 60% RH and 27+2°C for 72 h.

Transparency

The transparency of films was determined using a UV-1601 spectrophotometer (Shimadzu, Kyoto, Japan). The films sample were cut into rectangles and placed on the internal side of spectrophotometer cell. The transmittance of films was determined at 600 nm as described by Han and Floros (1997). The transparency of the films was calculated as follows:

$$\text{Transparency} = -\log T600/x$$

Where T600 is the transmittance at 600 nm and x is the film thickness (mm).

Thermogravimetric analysis (TGA)

Thermogravimetric analysis was performed to study the degradation characteristic of the films. Thermal stability of each sample was determined using a (PerkinElmer, TGA7) with a heating rate of 10°C/min in a nitrogen environment. It has a weighing capacity of 1.0 g. Samples were heated from room temperature to 500°C.

Differential scanning calorimetry (DSC)

The DSC analysis was determined using

a modulated differential scanning calorimeter (PerkinElmer, DSC7) with refrigerator cooler. Calibration was based on pure indium and sapphire. An empty Aluminum pan was used as reference. Samples (0.03 g) were scanned at a rate of 10°C/min between temperature ranges of -50°C to 220°C. The glass transition temperatures were determined from the resulting thermograms as the midpoint between onset and end temperatures of step changes in heat flow observed during heating and identified as second-order transitions.

Dynamic mechanical thermal analysis (DMTA)

The small deformation analysis of the films was performed in tension in a dynamic mechanical thermal analyzer (Rheometric Scientific, DMTA V). The tested filmstrips were cut into small strips (20 × 5 mm) and clamped in the instrument with the initial grip separation 5.5 mm. The films were subjected to a sinusoidal strain on top of a static deformation. The testing was conducted at a constant frequency of 1 Hz and a strain of 0.02% and over a temperature range of 50 to 200°C, at a heating rate of 5°C /min. The measurements of each experimental point were done at least in triplicates. When dynamic mechanical spectroscopy is employed within the linear viscoelastic regime to determine Tg, the storage and loss modulus (E' and E'') and loss tangent (tanδ = ΔE'/E'') are measured as a function of temperature at a constant frequency and a selected heating or cooling rate.

Statistical aenalysis

A factorial design was used to characterize the composite films. Analysis of variance (ANOVA) was used to compare mean differences of the samples. If the differences in mean existed, multiple comparisons were performed using Duncan's Multiple Range Test (DMRT).

Results and Discussion

FTIR spectroscopy of untreated and treated PPF

FTIR spectra for the untreated PPF and silane treated PPF is shown in Figure 1, a strong and broad absorption was found at 3335 cm^{-1}. This implies the presence of –OH groups in the fibers and hydrogen bonding between those –OH groups. However, the absorption peak of –OH groups for the silane treated PPF was shifted to a higher wave number near 3400 cm^{-1}. This implies that the degree of hydrogen bonding between –OH groups was decreased, and the absorption peak of –OH groups was shifted to the position of free –OH groups (higher wave number)

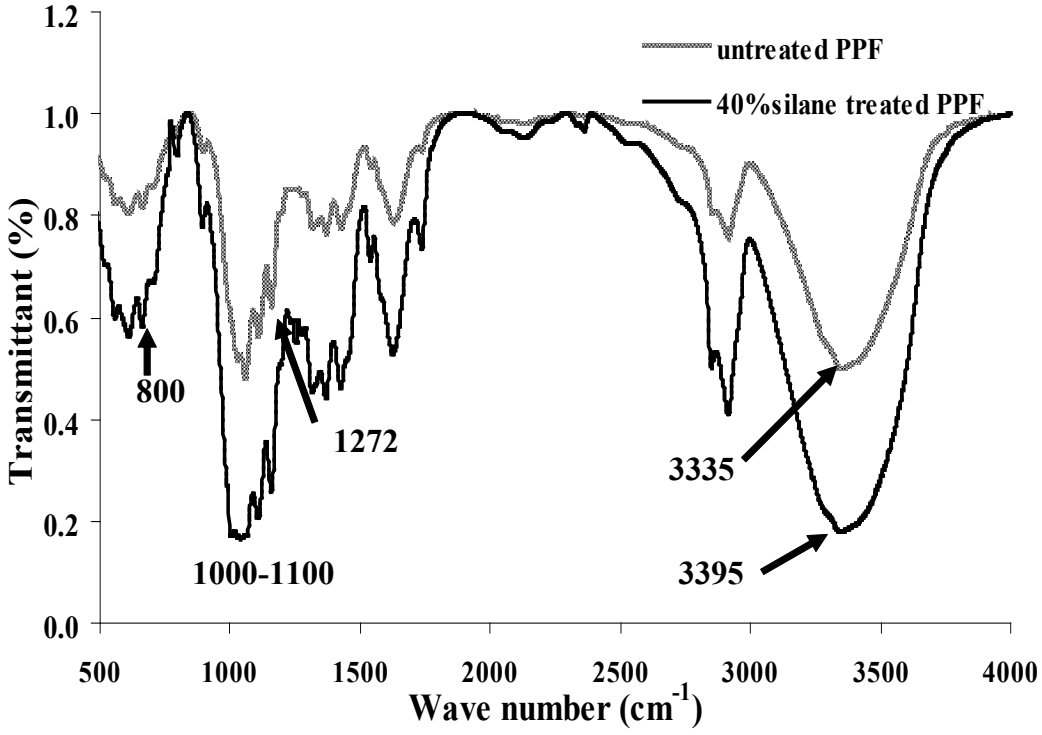

Figure 1. Fourier Transform Infrared (FTIR) spectra for the untreated PPF and 40% silane treated PPF.

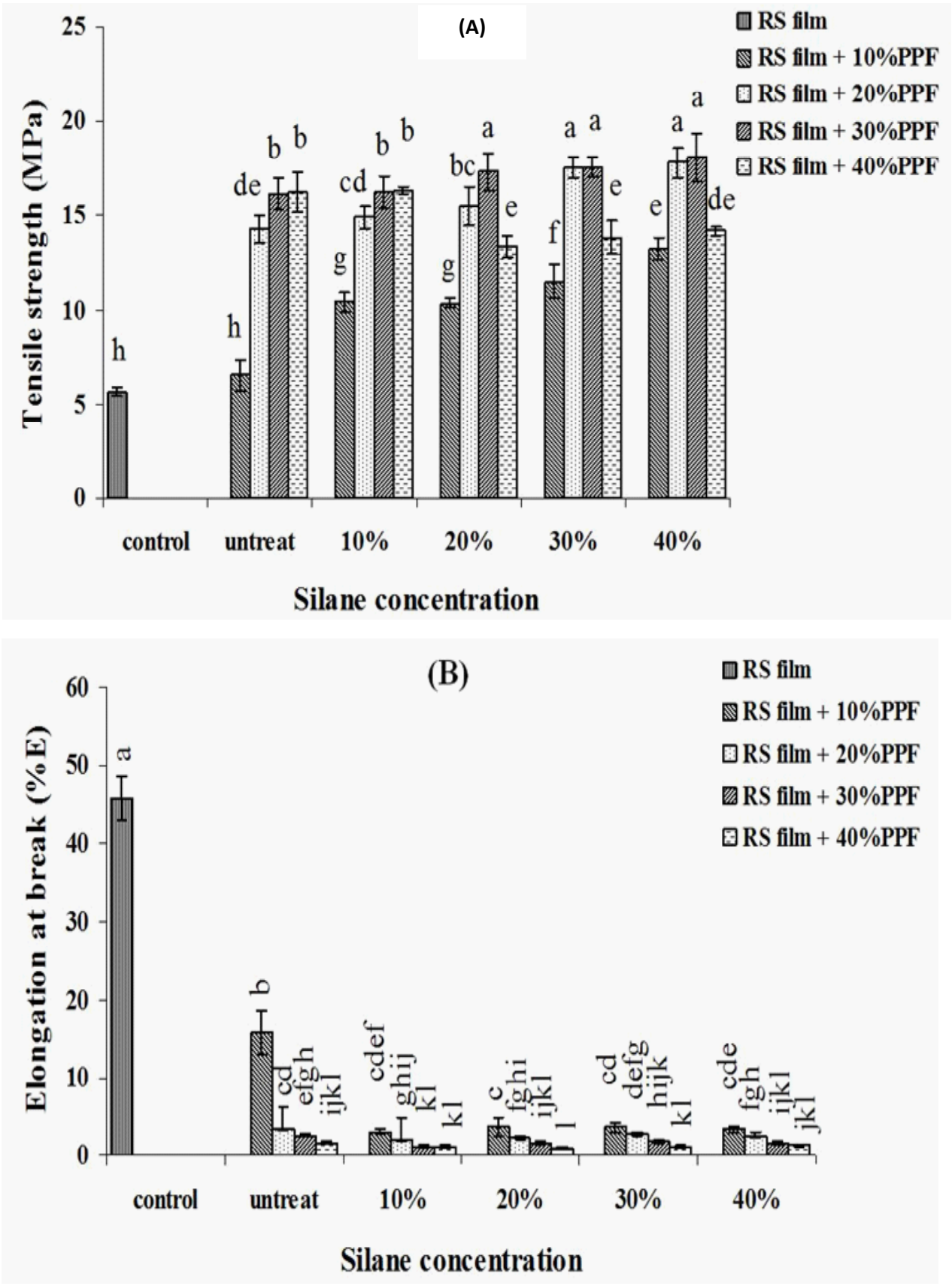

Figure 2. Effect of silane fiber surface treatment on tensile strength (A) and elongation at break (B) of RS films. Mean values with different letter are significantly different ($p<0.05$).

(Shih, 2006). Moreover, the characteristic absorption peaks of epoxide at 800 and 1272 cm^{-1} were found for silane coupling agent (glysidoxyproply trimethoxy silane). Furthermore, a slight increment in the broadness around 1000-1100 cm^{-1} was found for the silane treated PPF. This could be attributed to the presence of the asymmetric stretching of -Si-O-Si- and/or –Si-O-C- bonds. Which is in agreement with the results reported by Herrera-Franco and Valadez-Gonzalez (2005), the broad intense bands around 1200 was assigned to the stretching of the –Si-O-cellulose. The former bond is indicative of the existence of silica deposited on the fibers, whereas the latter would confirm the occurrence of a condensation reaction between the silane coupling agents and the fibers.

Tensile strength (TS) and elongation at break (E)

The mechanical properties of the rice starch (RS) films reinforced with palm pressed fiber (PPF) or RS/PPF biocomposite films, such as tensile strength (TS) and elongation at break (E) is depicted in Figure 2. The importance of the silane treatment can be assessed by comparing the results of the RS films contained untreated and silane treated PPF. Figure 2a. Illustrates the TS of RS films containing the untreated and silane treated PPF (10 - 40% silane coupling agents). In the same amount of PPF fillers, the TS of RS films contained silane treated PPF was higher than the RS films contained untreated PPF films. This is in agreement with the results reported by Herrera-Franco and Valadez-Gonzalez (2005) for composites with henequen fibers were treated with vinyltris silane and HDPE matrix. Moreover, the TS of RS films contained untreated and silane treated PPF increased as the PPF content increased (Figure 2a), indicated that a high compatibility occurs between starch matrix and PPF fillers and the performances (e.g., mechanical properties). Besides, at lower fiber content dispersion of fiber is very poor so that TS was not occurred properly. Similar results were observed by Sreekumar et al., (2007) and Sangthong et al., 2009. However, superfluous filler was easy to congregate and increased porous on films such as the TS decreased at 40% PPF content of RS film. Similar results were observed by Pickering et al. (2003) reported that at the highest fiber percentages, an actual reduction in strength was observed. One explanation for the general reduction in the strength for the treated wood fiber as the fiber weight percentage increases could be related to fiber agglomeration, which would be more likely at higher fiber contents. Fiber – fiber interaction from hydrogen bonding is considered to be a significant barrier to fiber dispersion (Matuana et

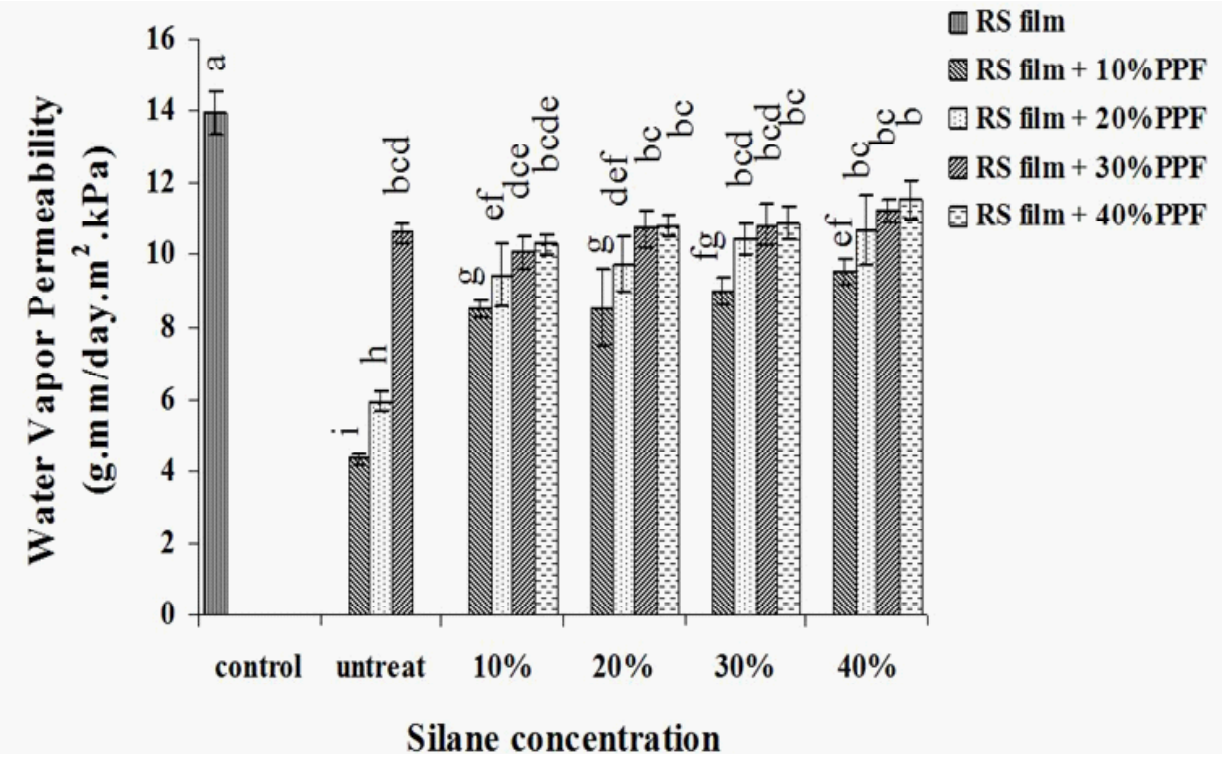

Figure 3. Effect of silane fiber surface treatment on water vapor permeability of RS films. Mean values with different letter are significantly different ($p<0.05$).

al., 1999). Concentration of silane coupling agent also affected the TS of RS films, the result showed that, TS tended to increase as concentration of silane coupling agent increase from 10 to 40%. The increased in the TS with an increased of silane concentration can be explained by the better adhesion between the filler and the matrix. Without silane coupling agent, the only adhesion mechanism is inter-diffusion. Silane coupling agents yields to hydrogen and covalent bonding between hydroxyl groups of filler and polysiloxanes formed by hydrogenation of silanes providing better adhesion between the fiber and the matrix. Better adhesion improves stress transfer through fibers, therefore, increases the TS of RS films (Demir et al., 2006). Abdelmouleh et al. (2004) point out the adsorption isotherns of silane onto the surface of fiber revealed that the same prehydrolysed silanes used here were adsorbed onto the surface of cellulosic fibers. This adsorption followed a mono- and multi-layer processes depending on the ratio between the quantity of the silane and that of the substrate. This adsorption was essentially driven by the formation of hydrogen bonds between the hydroxyl groups borne at the end of the short aliphatic moiety of the silane structure also contributed to the adsorption process through specific interactions. Regarding the Elongation at Break (E), silane concentration was not significantly affected on the E but there was affected by the PPF content; results demonstrated that increases in PPF fillers provided decrease in %E (Figure 2b). The experiments showed that TS and %E of RS films is almost inversely related. The decrease in the E due to the adhesion between fiber and matrix restricts deformation capacity of matrix in the elastic zone as well as the plastic zone (Demir et al., 2006). The experiments showed that TS and %E of RS films is almost inversely related.

Table 1. Char yields of RS films; RS film reinforced with untreated PPF and silane treated PPF (30% of starch).

Fiber/RS films	Char yield (%)
RS film	8.50 ± 0.52
RS film +untreated PPF	13.54 ± 0.78
RS film +10% Silane treated PPF	14.53 ± 0.67
RS film +20% Silane treated PPF	14.71 ± 0.92
RS film +30% Silane treated PPF	14.82 ± 0.41
RS film +40% Silane treated PPF	14.97 ± 0.25

Water vapor permeability (WVP)

As a food packaging, film is often required to avoid or at least to decrease moisture transfer between the food and the surrounding atmosphere, and water vapor permeability should be as low as possible (Ma et al., 2008). The results demonstrated that RS films contained 40% untreated PPF was broken during measuring the water vapor permeability, resulted from the occurring of brittle films. Water vapor permeability (WVP) of the RS composite films decreased with the addition of untreated and silane treated PPF, and the highest occurred when no fiber was added (14.15 g.mm/m2.day.kPa) but the lowest value (4.27 g.mm/m2.day.kPa) being obtained with addition of untreated PPF (Figure 3), this results pointed out that water resistance of PPF was better than rice starch matrix. WVP of the RS biocomposite films increased with the addition of silane treated PPF compared with RS films contained untreated PPF. However, the results showed that concentration of silane coupling agent did not significant effect on the WVP of treated RS biocomposite films. Water absorption in cellulose fibers is caused by hydrogen bonding between free hydroxyl groups on cellulose molecules and water molecules. Silane coupling agents form hydrogen or covalent bonds with some of free hydroxyl groups of cellulose, which reduce the water absorbtion capacity of cellulose (Sreekala and Thomas, 2003; Demir et al., 2006) but inversely in this research, WVP of the RS biocomposite films increased with the addition of silane treated PPF. It could be explained that R-group of silane coupling agents was hydrophilic properties, then superfluous silane was easy to interaction with water in surrounding atmosphere yielded the increasing of WVP of resulted films. WVP of the RS films tended to increase as content of untreated and silane treated PPF increased (Figure 3). The addition of PPF probably introduced a tortuous path for water molecule to pass through (Kristo and Biliaderis, 2007). At a low content of filler, PPF dispersed well in the rice starch matrix, and blocked the water vapor. However, superfluous filler was easy to congregate and increased porous on films, which actually decreased the effective contents of fiber and facilitated the water vapor permeation (Ma et al., 2008). Additionally, as the fiber content increased the water absorption also increased due to the increased hydrophilic nature of the fibers. Moreover, large number of porous tubular structures present in fiber accelerates the penetration of water by the so-called capillary action (Sreekumar et al., 2007). Similar trend is observed in for the composites prepared by Espert et al., (2004).

Color and transparency

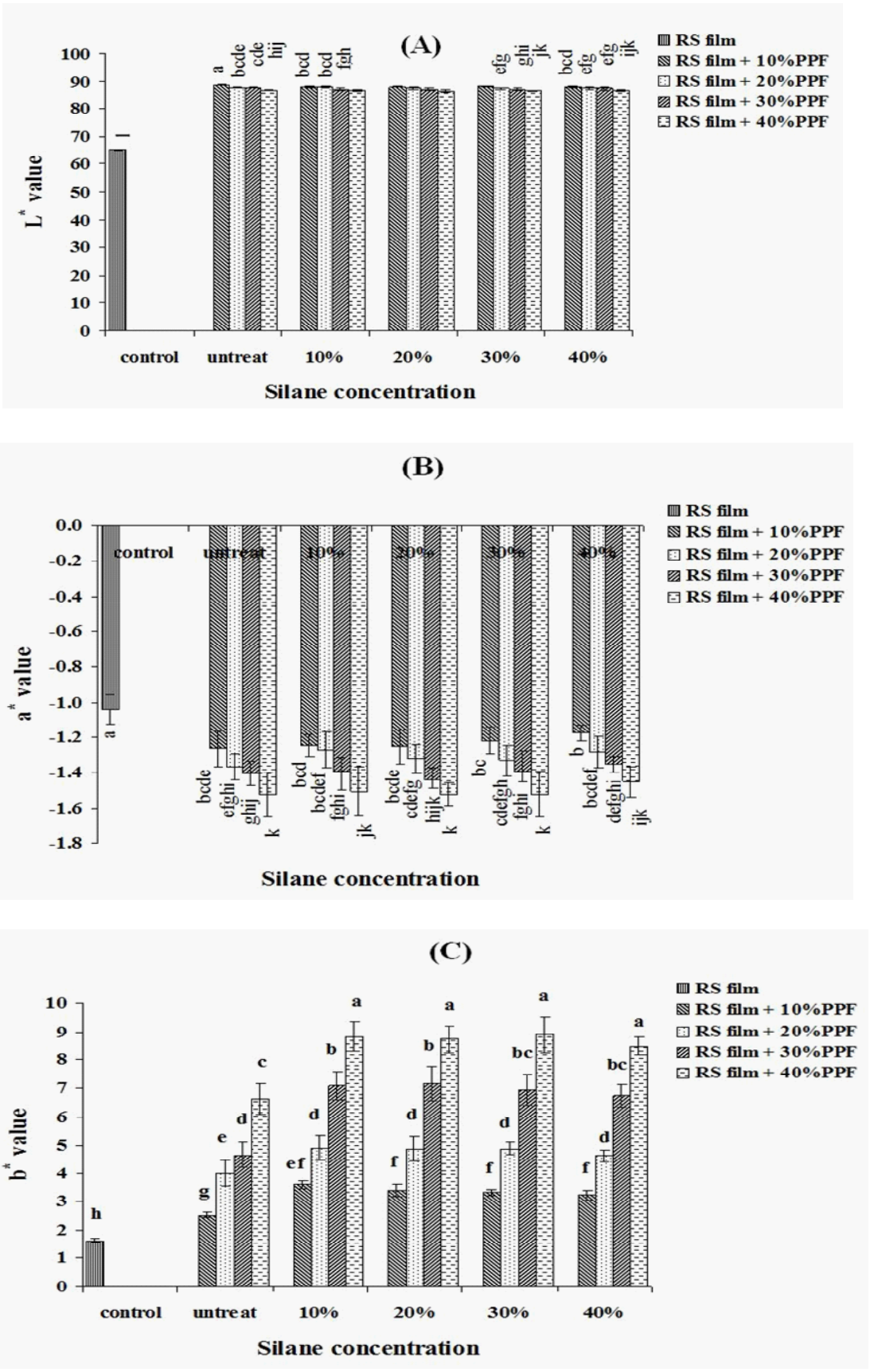

Figure 4. Effect of silane fiber surface treatment on L* (A); a* (B) and b* (C) of RS films. Mean values with different letter are significantly different ($p<0.05$).

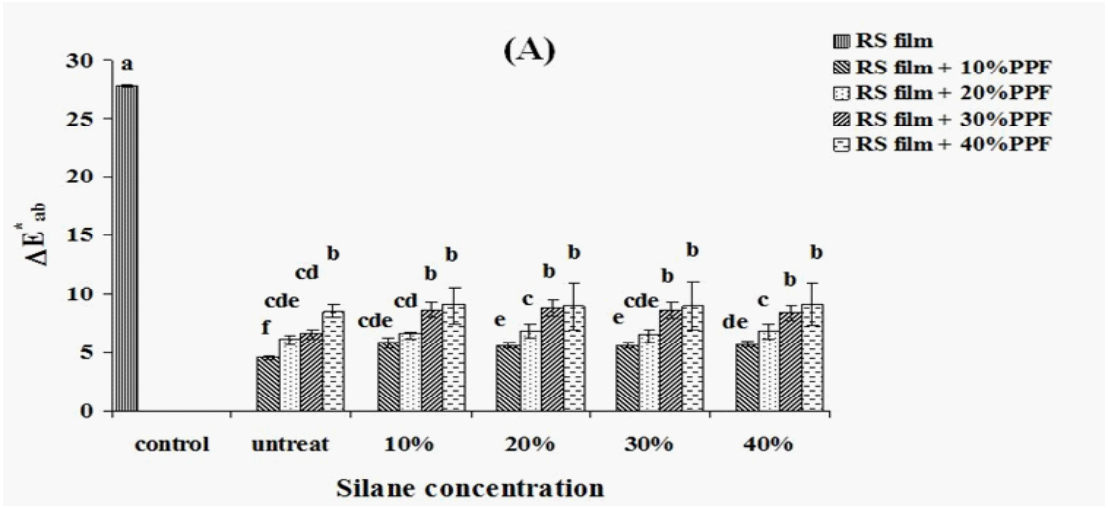

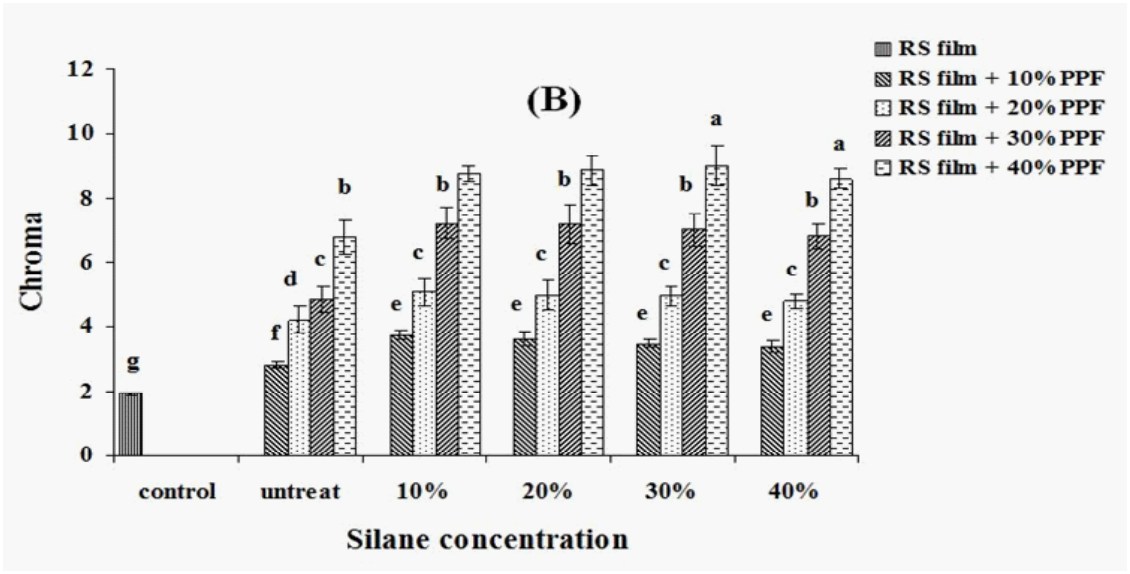

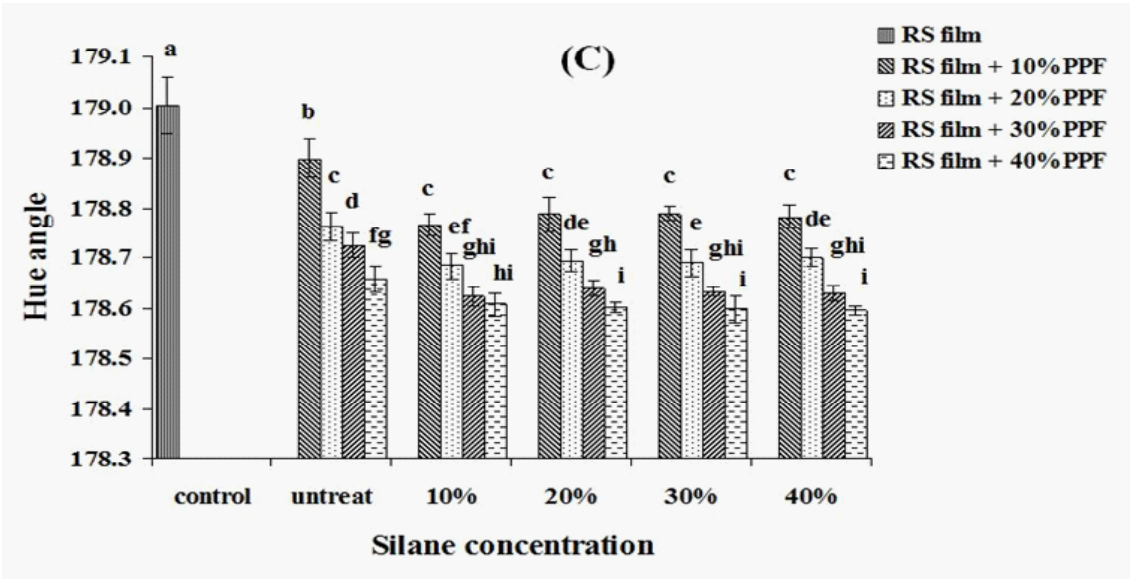

Figure 5. Effect of silane fiber surface treatment on ΔE* (A); Hue angle (B) and Chroma (C) of RS films. Mean values with different letter are significantly different ($p<0.05$).

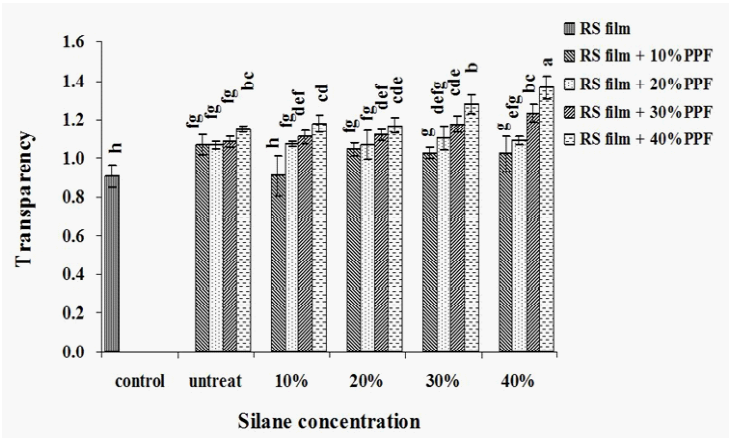

Figure 6. Effect of silane fiber surface treatment on transparency of RS films. Mean values with different letter are significantly different ($p<0.05$).

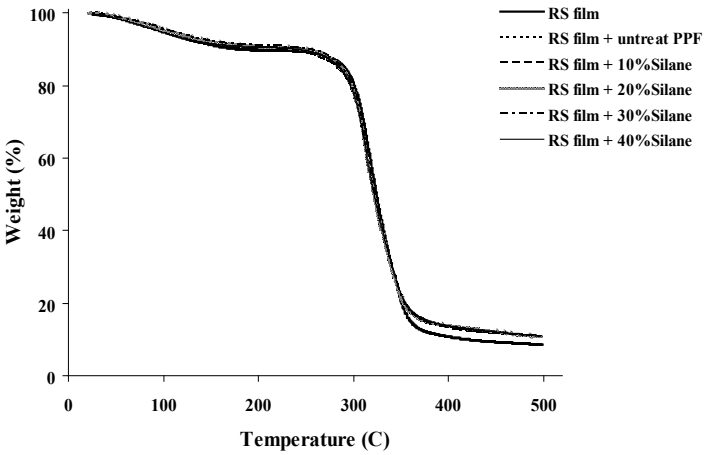

Figure 7. TGA thermograms of RS films and 0-40% silane treated PPF reinforced RS films.

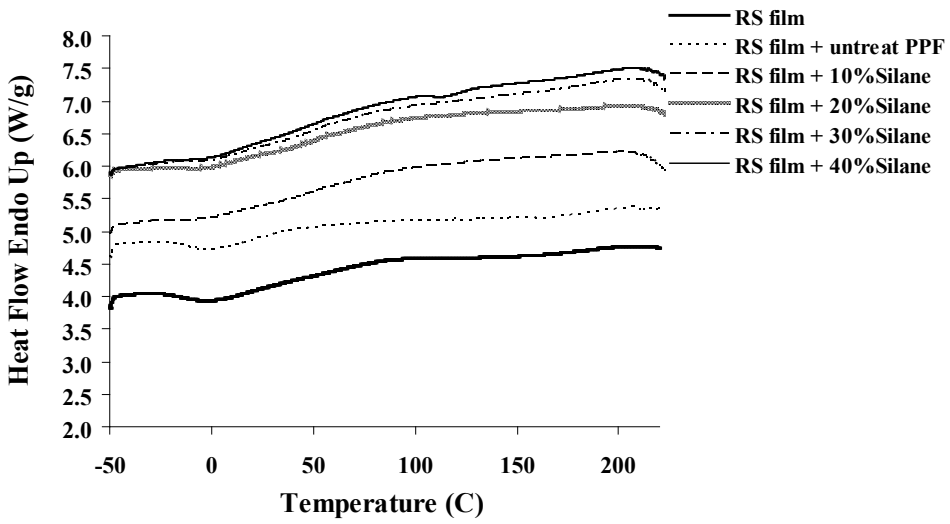

Figure 8. DSC curves of RS films and 0-40% silane concentration of PPF reinforced RS films.

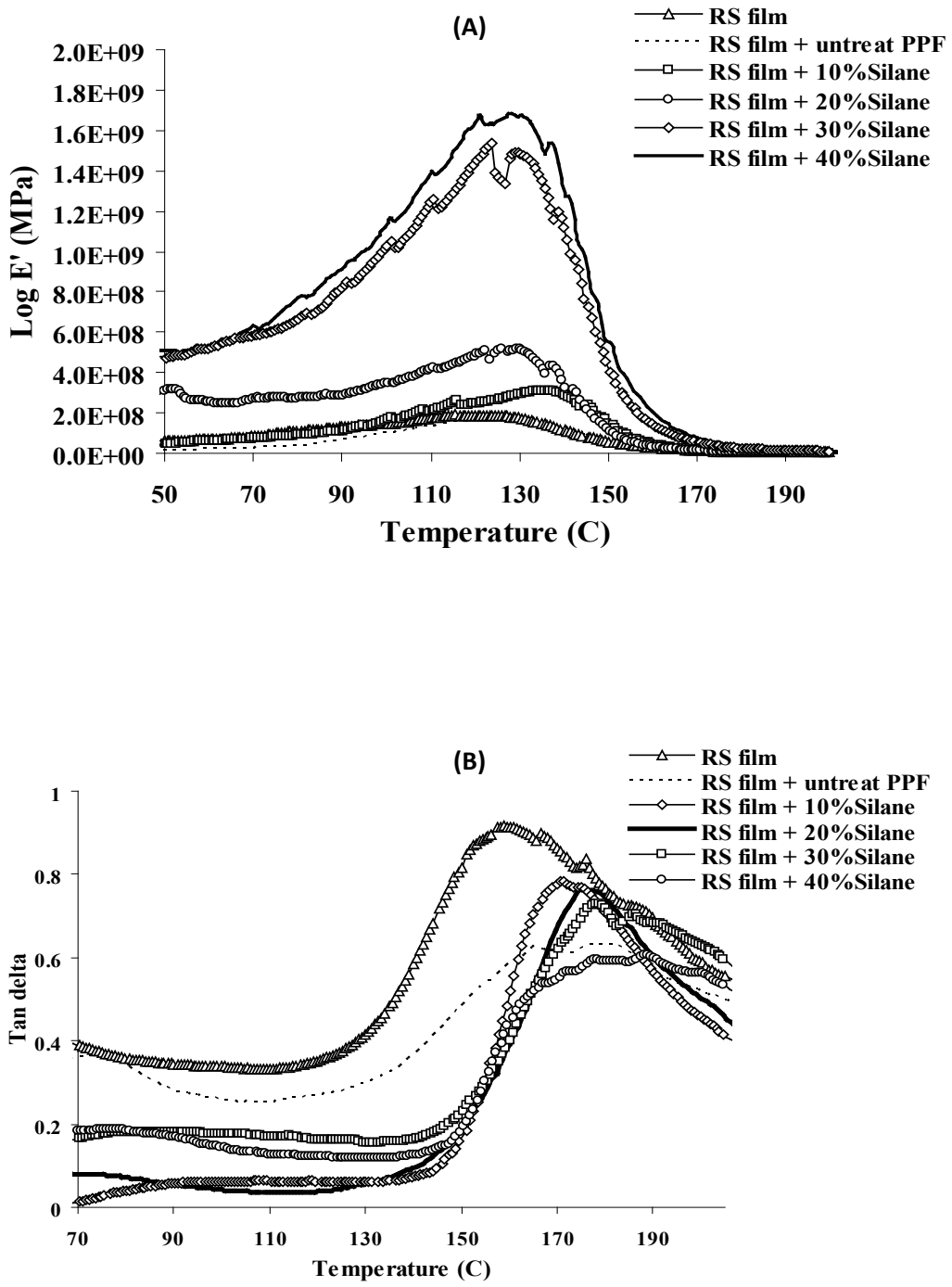

Figure 9. The dynamic mechanical behaviors of both (a) storage modulus (E') and (b) loss factor (tan δ) as a function of temperature for of RS films and 0-40% silane treated PPF reinforced RS films.

The results of the measurements performed on the RS film's color were expressed in accordance with CIELAB system and the rectangular coordinates (L*, a* and b*) and the total color difference (ΔE*ab), hue angle and chroma were calculated. Figure 4 and 5 depicted results from the effect of PPF surface treatment and content of PPF fillers on color (L*, a*, b*, ΔE*ab, chroma and hue angle) of RS films. The b* value and chroma of the RS biocomposite films contained silane treated PPF was higher than RS films reinforced with untreated PPF, however the silane surface treatment did not significantly affect on L*, a*, ΔE*ab, and hue angle. This indicated the increasing yellowness (b* and chroma) of film, possibly due to silane coupling agents have yellowish color when the fibers were treated with coupling agent and were added to RS films. The content of PPF fillers significantly affected on the color of RS films. The b* chroma and ΔE*ab values increased as content of untreated and silane treated PPF increased from 10 to 40% of starch concomitant with decreased in L*, a* and hue angle values. This indicated the decreasing lightness (L*) and increasing yellowness (b* and chroma) of film, possibly due to the PPF have white-yellowish color. Transparency of the films is also of importance in some instances, when used as packaging materials. Addition of PPF fiber into the RS films resulted in decrease their transparency. The RS films with out PPF fiber showed the highest transparent. However, the lower transparency of the films was noticed when a greater amount of PPF was incorporated (Figure 6). The decrease in transparency could possibly arise from the light scattering from the retarding of light transmission of the PPF and RS/PPF films. At high level of PPF, the RS films demonstrated lower transparency than lesser PPF incorporation.

Thermogravimetric analysis (TGA)

TGA thermograms and the char yields (500°C) of various samples under nitrogen are shown in Figure 7. The behavior of the char yield curves was similar in the composites (Figure 7 and Table 1). The results demonstrated that addition of silane treated PPF showed little better thermal properties of RS films than untreated fiber. This difference was due to the good adhesion between RS films and fiber, the silane coupling agent like adhesive that increased adhesion between PPF and matrix (Park et al., 2006). Similar trend was observed in the composites prepared by Shih (2007). According to the results, found that the char yield of RS films was enhanced as PPF content increased. Shih (2007) reported that the char yield is directly correlated to the potency of flame retardation for the polymers. Increasing char formation can limit the production of combustible gases, decreased the exo-thermicity of the pyrolysis reaction, and inhibit the thermal conductivity of the burning materials.

Differential scanning calorimetry (DSC)

Figure 8 shows the DSC curves RS films; RS film reinforced with untreated and silane treated PPF. No endothermic peaks, assigned to the glass transition temperature (Tg) of RS films. However, it can be observed from the increasing of endothermic heat flow when PPF was added into RS films. The endothermic heat flows of RS films reinforced with silane treated PPF fibers was higher than RS films reinforced with untreated PPF. These results pointed that the silane coupling agent seems to perform better in improving the compatibility between fiber and starch, which reduces the flexibility of molecular chains of starch (Lu et al., 2006). Moreover, the results showed that increasing concentration of silane treated PPF tended to increase in endothermic heat flows of resulted RS films. It could be explained that the silane coupling agent could perform better compatibility between PPF fiber and starch matrix, which reduces the flexibility of molecular chains of starch (Lu et al., 2006).

Dynamic mechanical thermal analysis (DMTA)

The dynamic mechanical thermal properties of the RS film and the RS reinforced with untreated and silane treated PPF were studied by DMTA measurements. DMTA is a very suitable tool to investigate the viscoelastic properties of materials in a wide range of temperatures and does not only provide fundamental information at the molecular level, but also correlates results with those obtained from tensile testing (Alemdar and Sain, 2008). In all the cases, a PPF loading of 30% have been used. The storage modulus (E') of the RS films and the RS films reinforced with untreated and silane treated PPF films as a function of temperature is given in Figure 9a. The peak of the storage modulus (E') value occurs at the temperature range around 110°C to 140°C. The storage modulus of the RS films increased when the silane treated PPF were added to RS films compared to the RS reinforced with untreated PPF. It could be explained that the change in the molecular structure of the starch polymer by interaction with the organo functional group of the silane treated fiber. The organo functional group of the silane forms interpenetrating polymer networks with the starch matrix that can be believed to cause the change in the polymer structure (Pothan and Thomas, 2003). The molecular structure of the polymer profoundly affects the Tg (Aklonis and MacKnight, 1983). The results pointed out that concentration of silane coupling agents also affected

the E' of RS films, found that, E' tended to increase as silane concentration increased from 10 to 40% by the reason of silane coupling agents could be improved the thermal properties by the better adhesion between the filler and the matrix.

Figure 9b shows the tan δ curves of the RS film and RS film reinforced with untreated and silane treated PPF as function of temperature. The glass transition temperatures were estimated from the tan δ peaks. The results depicted that there is a broad peak in tan δ at around 148°C of pure RS film and the Tg increased when untreated PPF was added into RS films. Additionally, the peak of tan delta of RS film reinforced with untreated shifted from 166°C to 187°C when reinforced with silane treated PPF. Similar results were observed by Agrawal et al. (2000). According to the results, increasing concentration of silane resulted in increased Tg of RS films. These results indicate that the fiber treated by coupling agents exhibited better compatibility with the starch matrices than the untreated fibers. Eklind et al. (1997) had been reported on an interlayer model to simulate the dynamic mechanical properties of filled blends. The filler particles have been reported to be surrounded by an interlayer attached to the filler surface. This phenomenon could give rise to filler structure in the matrix able to alter the dynamic mechanical modulus (Ray et al., 2001).

Conclusions

The impact of fiber surface treatment was more significant, higher tensile strength (TS), water vapor permeability (WVP) and thermal properties of RS films were observed as silane treated fiber was applied. Increasing amount of silane treated fibers resulted in increased TS and WVP but decreased in E. The glass temperature (Tg) shifted towards higher temperatures with increasing concentration of coupling agents, which can be restriction of the mobility of starch chain due to the establishment of strong interactions between RS and silane treated PPF. The maximum improvement in the mechanical and thermal properties obtained for the 40% glysidoxy propyltriethoxy silane treated PPF reinforced RS films. These results revealed that the interfacial interactions improved the filler compatibility, mechanical and thermal properties.

Acknowledgements

The authors would like to express the financial support given by the Graduate School of Prince of Songkla University, Hat Yai, Thailand. The authors wish to thank the rice starch support provided by Bangkok Starch Industrial Co. Ltd. Finally the authors would also like to thank "Palm Oil Product and Technology Research Center (POPTEC)" and "Starch and Plant Fiber Research Unit (SPF-RU)" for financial and experimental support.

References

Abdelmouleh,M. ,Boufi,S., Belgacem,M.N., Duarte,A. P., Salah,A. B. and Gandini, A. 2004. Modification of cellulosic fibers with functionalized silanes: development of surface properties. International Journal of Adhesive Adhesion 24: 43-54.

Agrawal, R., Saxena,N. S., Sharma, K. B., Thomas, S. and Sreekala, M. S. 2000.Activation energy and crystallization kinetics of untreated and treated oil palm fiber reinforced phenol formaldehyde composites. Material Science Engineering Part A. 277: 77-82.

Aklonis, J. J. and Macknight, W. J. 1983.Introduction to polymer viscoelasticity. John Wiley. London.

Alemdar, A. and Sain, M. 2008. Biocomposites form wheat straw nanofiber: Morphology, thermal and mechanical properties. Composite Science Technology 68(2): 557-565.

Angles, M. N. and Dufresne, A. 2000. Plasticized/tunicin whiskers nanocomposites. 1. Structural analysis. Macromolecules 33:8344-8353.

Angles, M. N. and Dufresne, A. 2000. Plasticized/tunicin whiskers nanocomposites. Materials. 2 Mechanical behavior. Macromolecules 34:2921-2931.

American Society for Testing and Materials (ASTM). 1991. Standard test method for tensile properties of plastics. D638. In : ASTM. Annual Book of American Standard Testing Methods, Vol 15.09. Philadelphia, PA., pp. 159-171.

American Society for Testing and Materials (ASTM). 1993a. Standard practice for conditioning plastics and electrical insulating materials for testing: D618-61 (Reproved 1990). In : ASTM. Annual Book of American Standard Testing Methods, Vol 8.01. Philadelphia, PA., pp.146-148.

American Society for Testing and Materials (ASTM). 1993b. Standard test method for water vapor transmission rate through plastic film and sheeting using a modulated infrared sensor: D1249-90. In : ASTM. Annual Book of American Standard Testing Methods, Vol 15.09. Philadelphia, PA., pp.1168-1172.

Averous, L. and Boquillon, N. 2004. Biocomposites based on plasticized starch: thermal and mechanical behaviors. Carbohydrate Polymer 56: 111-122.

Bledzki, A. K. and Gassan, J. 1999. Composites reinforced with cellulose based fibers. Progress in Polymer Science 24: 221-274.

Bourtoom, T. and Chinnan, M. S. 2008. Preparation and properties of rice starch-chitosan edible blend film. LWT-Food Science and Technology 41: 1633-1641.

Curvelo, A. A. S., De Carvalho,A. J. F. and Agnelli, J. A. M. 2001. Thermoplastic starch- cellulosic fibers composites: Preliminary results. Carbohydrate Polymer 45: 183-188.

De Carvalho, A. J. F., Curvelo, A.A.S. and Agnelli, J. A. M. 2002. Wood pulp reinforced thermoplastic starch composites International Journal of Polymer Material 51: 647-660.

Demir,H., Atikler, U., Balkose, D. and Tihminlioglu, F. 2006. The effect of fiber surface treatments on the tensile and water sorption properties of polypropylene-luffafiber composites. Composite Part. A. 37: 447-456.

Dufresne, A., Dupeyre, D. and Vignon, M. R. 2000. Cellulose microfibrils from potato tuber cells: processing and characterization of starch-cellulose microfibril composites. Journal of Applied Polymer Science 76: 2080-2092.

Dufresne, A. and Vignon, M. R. 1998. Improvement of starch film performances using cellulose microfibrils. Macromolecules 31: 2693-2696.

Eklind, H., Maurer, F. H. J. and Steeman, P. A. M. 1997. Micromechanical and microdielectric transitions in P (S-g-EO) modified PPO/PMMA blends. Polymer 38: 1047-1055.

Espert, A., Vilaplana, F. and Karlsson, S. 2004. Comparison of water absorption in natural cellulosic fibers from wood and one-year crops in polypropylene composites and its influence on their mechanical properties. Composite Part A. 35: 1267-1276.

Fishman, M. L., Coffin, D. R. and Konstance, R. P. 2000. Extrusion of pectin/starch blends plasticizered with glycerol. Carbohydrate Polymer 41: 317-325.

Funke, U., Bergthaller, W. and Lindhauer, M. G. 1998. Processing and characterization of biodegradable products based on starch. Polymer Degradation 59:293-296.

Han, J. H. and Floros, J. D. 1997. Casting antimicrobial packaging films and measuring their physical properties and antimicrobial activity. Journal of Plastic Film Sheet 13: 287-298.

Herrera-Franco, P. J. and Valadez-Gonzalez, A. 2005. A. study of the mechanical properties of short natural-fiber reinforced composites. Composite. Part B Engineering 36:597-608.

Kester, J. J. and Fennema, O. R. 1986. Edible films and coatings: a review. Food Technology 40:47-59.

Kristo, E. and Biliaderis, C. G. 2007. Physical properties of starch nanocrytal- reinforced pullulan films. Carbohydrate Polymer 68: 146-148.

Lourdin, D., Vaiie, G. and Colonna, P. 1995. Della influence of amylase content on starch films and foams. Carbohydrate Polymer 27: 275-280.

Low, I.M., McGrath, M., Lawrence, D., Schmidt, P., Lane, J., Latella, B.A. and Sim,K.s. 2007. Mechanical and fracture properties of cellulose-fiber-reinforced epoxy laminates. Composite Part A. 38: 963-974.

Lu, Y., Weng, L. and Cao, X. 2006. Morphological, thermal and mechanical properties of ramie crystallites reinforced plasticized starch biocomposites. Carbohydrate Polymer 63: 1-7.

Ma, X., Chang, P. R. and Yu, J. 2008. Properties of biodegradable thermoplastic pea starch/carboxymethyl cellulose and pea starch/microcrystalline cellulose composites. Carbohydrate Polymer 72: 369-375.

Mali, S. and Grossmann, M. V. E. 2003. Effects of yam starch films on storability and quality of fresh strawberries. Journal of Agricultural and Food Chemistry 7005-7011.

Matuana, L. M., Balatinecz., J. J., Park, C. B. and Sodhi, R. N. S. 1999. X-ray photoelectron spectroscopy study of silane-treated newsprint-fibers. Wood Science and Technology 33: 259-270.

McHugh, T. H., Avena-Bustillos, R. and Krochta, J. M. 1993. Hydrophilic edible film: modified procedure for water vapor permeability and explanation of thickness effects. Journal of Food Science 58: 899-903.

Park, H. M., Li, X., Jin, C. Z., Park, C. Y., Cho, W. J. and Ha, C. S. 2002. Preparation and properties of biodegradable thermoplastic starch/clay hybrids. Macromolecular Materials and Engineering 287: 553-558.

Park, J. M., Quang, S. T., Hwang, B.S. and Deveries, K. L. 2006. Interfacial evaluation of modified Jute and Hemp Fibers/polypropylene (PP)-maleic anhydride polypropylene copolymers (PP-MAPP) composities using micromechanical technique and nondestructive acoustic emission. Composite Science and Technology 66: 2686-2699.

Pickering, K. L., Abdalla, A., Ji, C., McDonald, A. G. and Franich, R. A. 2003. The effect of silane coupling agents on radiate pine fibre for use in thermoplastic matrix composites. Composites Part A, 34, 915-926.

Pothan, L. A. and Thomas, S. 2003. Polarity parameters and dynamic mechanical behaviour of chemically modified banana fiber reinforced polyester composites. Composite Science and Technology 63: 1231-1240.

Ray, D., Sarkar, B. K., Rana, A. K. and Bose, N. R. 2001. The mechanical properties of vinylester resin matrix composite reinforced with alkali treated jute fibers. Composite. Paet A. 32: 119-127.

Rodriguez, M., Oses, J., Ziani, K. and Mate, J. I. 2006. Combined effect of plasticizers and surfactants on the physical properties of starch based edible films. Food Research International 39: 840-846.

Sangthong, S., Pongprayoon, T. and Yanunet, N. 2009. Mechanical property improvement of unsaturated polyester composite reinforced with admicellar-treated sisal fiber. Composite Part A: 40(6-7): 687-694.

Santayanon, R. and Wootthikanokkhan, J. 2003. Modification of cassava starch by using propionic anhydride and properties of the starch-based composite foams. Carbohydrate Polymer 51: 17-24

Shih, Y. F. 2007. Mechanical and thermal properties of waste water bamboo husk fiber reinforced epoxy composites. Material Science and Engineering Part A. 445-446: 289-295.

Sreekala, M. S. and Thomas, S. 2003. Effect of fiber of surface modification on water-sorption characteristics of oil palm fibers. Composite Science and Technolology 63:861-869.

Sreekumar, P. A., Joseph, K., Unnikrishnan, G. and Thomas S. 2007. A comparative Study on mechanical property of sisal leaf fiber reinforced polyester composites prepared by resin transfer and compression moulding techniques. Composite Science and Technology 67(3-4):453-461.

Wittaya, T. 2009. Microcomposites of rice starch film reinforced with microcrystalline cellulose from palm pressed fiber. International Food Research Journal 16: 493-500.

Xu, X. Y., Kim, K. M., Hanna, M. A. and Nag, D. 2005. Chitosan-starch composite film: preparation and characterization. Journal of Industrial Crops Products 21: 185-192.